

Synthesis and Characterization of the First Niobocene Germyl Complexes and Reactivity of Triphenylsilyl-, Triphenylgermyl-, and Triphenylstannylniobocene Derivatives. X-ray Molecular Structures of d^0 $Nb(\eta^5-C_5H_4SiMe_3)_2(H)_2(EPh_3)$ ($E = Ge, Sn$)

A. Antiñolo,[†] F. Carrillo-Hermosilla,[†] A. Castel,[‡] M. Fajardo,[§]
J. Fernández-Baeza,[†] M. Lanfranchi,^{||} A. Otero,^{*,†} M. A. Pellinghelli,^{||} G. Rima,[‡]
J. Satgé,[‡] and E. Villaseñor[†]

Departamento de Química Inorgánica, Orgánica y Bioquímica, Universidad de Castilla-La Mancha, Campus Universitario de Ciudad Real, 13071 Ciudad Real, Spain, Departamento de Química Inorgánica, Universidad de Alcalá, Campus Universitario, 28871 Alcalá de Henares, Spain, Dipartimento di Chimica Generale ed Inorganica, Chimica Analitica, Chimica Fisica, Università degli Studi di Parma, Centro di Studio per la Strutturistica Diffraattometrica del CNR, Viale delle Scienze 78, 43100 Parma, Italy, and Laboratoire de Chimie des Organominéraux-URA 477, Université Paul Sabatier, Route de Narbonne, 118, 31062 Toulouse Cedex, France

Received November 13, 1997

Thermal treatment of $Nb(\eta^5-C_5H_4SiMe_3)_2(H)_3$ (**1**) with the appropriate organogermanium hydrides ($HGeR_3$) and $HSnPh_3$ gives the corresponding niobocene germyl hydrides $Nb(\eta^5-C_5H_4SiMe_3)_2(H)_2(GeR_3)$, $GeR_3=GePh_3$ (**2**), $GePh_2H$ (**3**), $GeEt_3$ (**4**), $Ge(C_6H_{13})_3$ (**5**), Ge^iAm_3 ($iAm = CH_2CH_2CH(CH_3)_2$) (**6**), $Ge(C_6H_{13})_2Cl$ (**7**), Ge^iAm_2Cl (**8**), $Ge(C_6H_{13})_2H$ (**9**), Ge^iAm_2H (**10**), and $Nb(\eta^5-C_5H_4SiMe_3)_2(H)_2(SnPh_3)$ (**11**) in good yields. Spectroscopic data indicate the presence of only one of the two possible structural isomers in which the germyl or stannyl group is in the equatorial plane with a symmetrical structure. Reactivity studies on the series $Nb(\eta^5-C_5H_4SiMe_3)_2(H)_2(ER_3)$, $E = Si$ (**12**), Ge (**2**), Sn (**11**), were carried out. **12** reacts with H_2 to give **1**, but **2** and **11** were unreactive toward this reagent. Furthermore, a similar behavior was observed with CO and $CN(2,6-Me_2C_6H_3)$. Thus, **12** reacts with these reagents to give rise, after elimination of $HSiPh_3$, to $Nb(\eta^5-C_5H_4SiMe_3)_2(H)(CO)$ and $Nb(\eta^5-C_5H_4SiMe_3)_2(H)(CN(2,6-Me_2C_6H_3))$, respectively, while **2** and **11** do not react. Reactions of **12** with $HGePh_3$ and $HSnPh_3$ and of **2** with $HSnPh_3$ gave σ -bond metathesis products, but no reactions were observed between **2** and $HSiPh_3$ or between **11** and $HSiPh_3$ or **11** and $HGePh_3$. The kinetics of these processes have been studied by 1H NMR spectroscopy and indicated the following reactivity trends $Nb-SiPh_3 > Nb-GePh_3 > Nb-SnPh_3$ for the different processes considered. The X-ray molecular structures of **2** and **11** were established by diffraction studies. The two isostructural complexes show a bent-sandwich coordination with the two hydrides flanking either side of the Nb–Ge and Nb–Sn bonds (2.710(1), 2.830(1) Å in **2** and **11**, respectively).

Introduction

Early transition metal d^0 complexes containing bonds with group 14 elements have received special attention in the past few years. In particular, research on d^0 metal silyl complexes has revealed a number of interesting reactivity patterns, such as migratory insertions of unsaturated substrates into metal–silicon bonds¹ and σ -bond metathesis processes.² In recent years, there has been mounting evidence that the oxidative addition of organosilicon hydrides to coordinatively unsaturated hydride group 5 metal complexes is a successful method for preparing d^0 metal complexes.³ Using this method,

we recently prepared⁴ several niobocene silyl complexes $Nb(\eta^5-C_5H_4SiMe_3)_2(H)_2(SiR_3)$. We wanted to prepare a series of metallocene niobium derivatives with silyl, germyl, and stannyl ligands to compare their chemical

(1) Selected references: (a) Campion, B. K.; Falk, J.; Tilley, T. D. *J. Am. Chem. Soc.* **1987**, *109*, 2049. (b) Arnold, J.; Tilley, T. D. *J. Am. Chem. Soc.* **1987**, *109*, 3318. (c) Elsner, F. H.; Tilley, T. D.; Rheingold, A. L.; Geib, S. J. *J. Organomet. Chem.* **1988**, *358*, 169. (d) Arnold, J.; Tilley, T. D.; Rheingold, A. L.; Geib, S. J.; Arif, A. M. *J. Am. Chem. Soc.* **1989**, *111*, 149. (e) Roddick, D. M.; Heyn, R. H.; Tilley, T. D. *Organometallics* **1989**, *8*, 324. (f) Arnold, J.; Engeler, M. P.; Elsner, F. H.; Heyn, R. H.; Tilley, T. D. *Organometallics* **1989**, *8*, 2284. (g) Campion, B. K.; Heyn, R. H.; Tilley, T. D. *J. Am. Chem. Soc.* **1990**, *112*, 2011. (h) Woo, H.-G.; Tilley, T. D. *J. Organomet. Chem.* **1990**, *393*, C6. (i) Campion, B. K.; Heyn, R. H.; Tilley, T. D. *Inorg. Chem.* **1990**, *29*, 4355.

(2) Selected references: (a) Tilley, T. D. *Inorg. Chem.* **1990**, *10*, 37. (b) Harrod, J. F.; Mu, Y.; Samuel, E. *Polyhedron* **1991**, *11*, 1239. (c) Corey, J. *Advances in Silicon Chemistry*; Larson, G., Ed.; JAI Press: Greenwich, CT, 1991; Vol. 1, p 327.

[†] Universidad de Castilla-La Mancha.

[‡] Université Paul Sabatier.

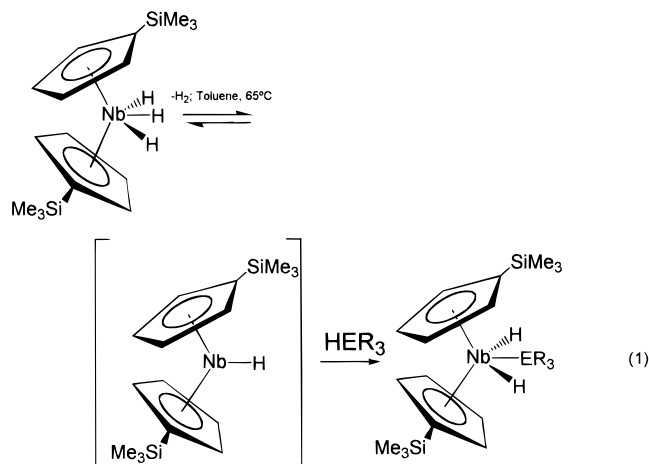
[§] Universidad de Alcalá.

^{||} Università degli Studi di Parma.

and physical properties. For the niobocene chemistry, Green et al.⁵ prepared the stannyl complexes $\text{Nb}(\eta^5\text{-C}_5\text{H}_5)_2(\text{H})_2(\text{SnR}_3)$ by reaction of $[\{\text{Nb}(\eta^5\text{-C}_5\text{H}_5)_2(\text{H})_2\text{Li}\}]$ with the appropriate SnR_3Cl reagents. To complete the series of analogous d^0 niobocene silyl, germyl, and stannyl complexes we have started studies focused on the preparation of the corresponding d^0 niobocene germyl derivatives. Here, we report the results concerning the synthesis and characterization of the first niobocene germyl complexes $\text{Nb}(\eta^5\text{-C}_5\text{H}_4\text{SiMe}_3)_2(\text{H})_2(\text{GeR}_3)$ as well as the reactivity trends for a series of analogous $\text{Nb}(\eta^5\text{-C}_5\text{H}_4\text{SiMe}_3)_2(\text{H})_2(\text{EPh}_3)$ ($\text{E} = \text{Si, Ge, Sn}$) complexes in hydrogenolysis and σ -bond metathesis reactions.

Results and Discussion

The reaction between $\text{Nb}(\eta^5\text{-C}_5\text{H}_4\text{SiMe}_3)_2(\text{H})_3$ (**1**) and several organogermanium hydrides, HGeR_3 , and HSnPh_3 in toluene at 65 °C gives the corresponding monogermyl and -stannyl complexes (eq 1), $\text{GeR}_3\text{=GePh}_3$ (**2**), GePh_2H (**3**), GeEt_3 (**4**), $\text{Ge}(\text{C}_6\text{H}_{13})_3$ (**5**), Ge^iAm_3 ($i\text{Am} = \text{CH}_2\text{CH}_2\text{CH}(\text{CH}_3)_2$) (**6**), $\text{Ge}(\text{C}_6\text{H}_{13})_2\text{Cl}$ (**7**), $\text{Ge}^i\text{Am}_2\text{Cl}$ (**8**), $\text{Ge}(\text{C}_6\text{H}_{13})_2\text{H}$ (**9**), $\text{Ge}^i\text{Am}_2\text{H}$ (**10**) and SnPh_3 (**11**). The



reaction may proceed via reductive elimination of H_2 to give the 16e coordinatively unsaturated $\text{Nb}(\eta^5\text{-C}_5\text{H}_4\text{-SiMe}_3)_2\text{H}$ complex and subsequent oxidative addition of HER_3 to give a closed-shell 18e configuration in the germyl and stannyl dihydride derivatives. This method was previously employed in the synthesis of several tantalocene silyl hydride derivatives^{3b,d,e} and some related niobocene hydride complexes.^{3b,f,4} Complexes **2–11** were isolated as air-sensitive microcrystalline materials. No reaction was observed between **1** and $\text{HGe}(\text{mes})_2\text{H}$, $\text{mes} = 2,4,6\text{-trimethylphenyl}$, even when the reaction mixture was refluxed in toluene for several hours. We propose that the more sterically demanding germyl moiety should encounter greater steric hin-

drance in its approach to the metal center in the oxidative addition of the organogermanium hydride reagent. Similarly, the diorganogermanium hydride $(\text{HGe}(\text{mes})_2)_2$ containing a Ge–Ge bond did not react with **1** in refluxing toluene. As far as we know, this is the first time that d^0 early transition metal germyl complexes have been prepared by oxidative addition of organogermanium hydrides to coordinatively unsaturated hydride substrates. Previously, several germyl derivatives of the group 4 metals, actinides, or scandium have been described⁶ by reaction of germyllithium reagents with the appropriate haloderivatives. Complexes **2–11** were characterized spectroscopically. The NMR data suggest that only the symmetrical isomer of these complexes is present in solution. The cyclopentadienyl rings are equivalent, showing two broad resonances (see Experimental Section) for an A_2B_2 spin system in the ^1H NMR spectra, which indicates a symmetrical disposition on the niobium center with a rapid rotation of the ER_3 moiety around the Nb–E bond. In addition, the ^{13}C NMR spectra show the three expected resonances for the cyclopentadienyl carbon atoms (see Experimental Section). We conclude that the thermodynamically more favorable symmetrical isomer (see eq 1) was obtained for all of the germyl and stannyl complexes. Similar NMR spectral behavior was found for the analogous niobocene silyl complexes.⁴ The IR spectra of **2–11** show $\nu(\text{Nb–H})$ at ca. 1750 cm^{-1} , and in addition, the spectra of **3, 9**, and **10**, which contain hydrogen on the germyl moieties, exhibit $\nu(\text{Ge–H})$ as a medium-sized intensity band at ca. 1900 cm^{-1} (see Experimental Section). The ^1H NMR spectra show resonances due to the hydride ligands at ca. -4.0 ppm as broad signals, and these values are at similar chemical shifts as those reported for the equivalent hydride ligands in $\text{Nb}(\eta^5\text{-C}_5\text{H}_4\text{SiMe}_3)_2(\text{H})_2(\text{SiR}_3)$ ⁴ ($\text{SiR}_3 = \text{SiPh}_3$ (**12**)). On the basis of the ^{29}Si NMR data, we established the classical nature of these silyl hydrides. In the germyl and stannyl complexes, both the NMR and the structural data support a classical or nonclassical hydrido germyl or stannyl structure. Solid-state X-ray molecular structure determination of complexes **2** and **11** was carried out. Views of complexes **2** and **11** are shown in Figure 1 together with the atomic-numbering scheme. Selected bond distances and angles are listed in Table 1. The coordination around the Nb atom can be described as a distorted tetrahedron with the vertices occupied by the two Cp' ring centroids and the two hydrides. The E atom interacts ($\text{Nb–Ge} = 2.710(1)\text{ \AA}$, $\text{Nb–Sn} = 2.830(1)\text{ \AA}$) with the Nb atom, roughly bisecting the H1T–Nb–H2T angle ($\text{H1T–Nb–H2T} = 107(3)^\circ$, $\text{Ge–Nb–H1T} = 56(2)^\circ$, and $\text{Ge–Nb–H2T} = 51(2)^\circ$ in **2** ($\text{H1T–Nb–H2T} = 120(3)^\circ$, $\text{Sn–Nb–H1T} = 65(2)^\circ$, and $\text{Sn–Nb–H2T} = 55(2)^\circ$ in **11**). The coordination environment is of pseudo- C_2 symmetry with the 2-fold axis passing through the Nb–E bond. This coordination is very similar to that found in the parent $\text{Nb}(\eta^5\text{-C}_5\text{H}_4\text{SiMe}_3)_2(\text{H})_2(\text{SiPh}_2\text{H})$,⁴ with pseudo- C_2 symmetry, and in $\text{Nb}(\eta^5\text{-C}_5\text{H}_5)_2(\text{H})_3$ ⁷ with pseudo- C_s symmetry. The Nb–CE distances in **2** and **11** compare well with those reported for the latter two compounds

(3) (a) Allison, J. S.; Aylett, B. J.; Colquhoun, H. M. *J. Organomet. Chem.* **1976**, *112*, 67. (b) Curtis, M. D.; Bell, L. G.; Buttler, W. M. *Organometallics* **1985**, *4*, 701. (c) Berry, D. H.; Jiang, Q. *J. Am. Chem. Soc.* **1987**, *109*, 6211. (d) Aitken, C.; Barry, J. P.; Gauvin, F.; Harrod, J. F.; Malek, A.; Rousseau, D. *Organometallics* **1989**, *8*, 1732. (e) Jiang, Q.; Carroll, P. J.; Berry, D. H. *Organometallics* **1991**, *10*, 3648. (f) Green, M. L. H.; Hughes, A. K. *J. Organomet. Chem.* **1996**, *506*, 221.

(4) Antiñolo, A.; Carrillo, F.; Fajardo, M.; Otero, A.; Lanfranchi, M.; Pellinghelli, M. A. *Organometallics* **1995**, *14*, 1518.

(5) (a) Green, M. L. H.; Hughes, A. K.; Mountford, P. *J. Chem. Soc., Dalton Trans.* **1991**, 1407. (b) Green, M. L. H.; Hughes, A. K.; Mountford, P. *J. Chem. Soc., Dalton Trans.* **1991**, 1699.

(6) (a) Kingston, B. M.; Lappert, M. F. *J. Chem. Soc., Dalton Trans.* **1972**, 69. (b) Nolan, S. P.; Porchia, M.; Marks, T. J. *Organometallics* **1991**, *10*, 1450. (c) Woo, H.-G.; Freeman, W. P.; Tilley, T. D. *Organometallics* **1992**, *11*, 2198.

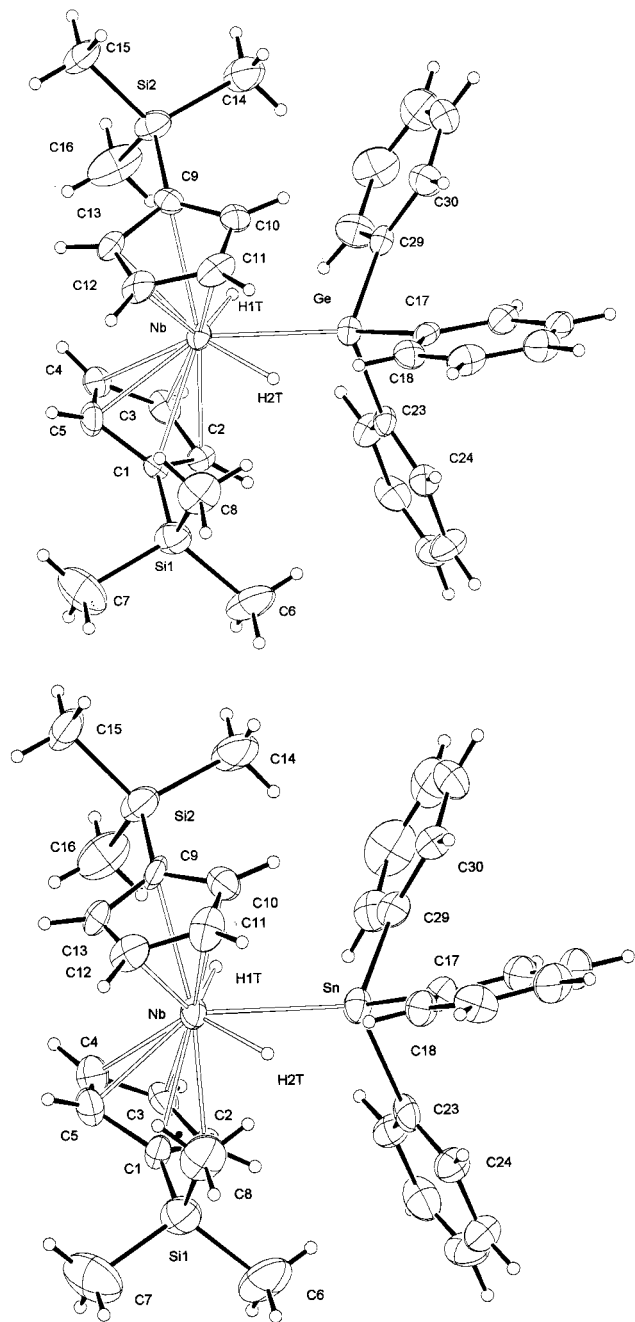


Figure 1. ORTEP drawings of complexes **2** (a, top), and **11** (b, bottom), with the atomic-labeling scheme. The thermal ellipsoids are at the 30% probability level.

with the 3 esd criteria. The Nb, E, H1T, and H2T atoms are coplanar (maximum deviation 0.04(5) Å for H2T in **2** and 0.0032(8) Å for Nb in **11**), and their weighted least-squares plane is almost perpendicular to the plane defined by the Nb atom and the two centroids of the Cp' rings (91(1)° (**2**) and 92(1)° (**11**)). The two bent Cp' rings, which are nearly staggered (mean torsion angles values 28.3(8)° (**2**) and 27.4(10)° (**11**)) with the two SiMe₃ groups trans to each other, form a dihedral angle of 42.8(3)° (**2**) and 41.8(4)° (**11**) and are bound to the Nb atom in the symmetric conventional η^5 -fashion (Nb–C_{p'} ranges 2.375(8)–2.411(7), 2.375(8)–2.423(8) Å in **2** and 2.350(10)–2.418(9), 2.366(9)–2.427(9) Å in **11**). The two hydride ligands were clearly located in each structure, and the Nb–H bond lengths (1.58(5), 1.69(6) Å in **2** and 1.62(5), 1.72(6) Å in **11**), which fall in the

Table 1. Selected Bond Distances (Å) and Angles (deg) (with Esd's in Parentheses) for Compounds **2** and **11**^a

	2	11
Nb–CE1	2.074(7)	2.064(9)
Nb–CE2	2.078(7)	2.074(8)
Nb–H1T	1.58(5)	1.62(5)
Nb–H2T	1.69(6)	1.72(6)
Nb–E	2.710(1)	2.830(1)
E–C17	2.000(8)	2.128(9)
E–C23	2.000(8)	2.192(10)
E–C29	1.976(8)	2.177(10)
Si1–C1	1.861(8)	1.839(10)
Si1–C6	1.863(10)	1.836(11)
Si1–C7	1.856(10)	1.842(11)
Si1–C8	1.875(8)	1.860(11)
Si2–C9	1.859(9)	1.849(10)
Si2–C14	1.852(9)	1.865(11)
Si2–C15	1.868(9)	1.841(10)
Si2–C16	1.847(8)	1.812(10)
E···H1T	2.24(5)	2.59(5)
E···H2T	2.11(6)	2.31(6)
CE1–Nb–CE2	138.1(3)	139.5(4)
CE1–Nb–H1T	100(2)	101(2)
CE1–Nb–H2T	104(2)	106(2)
CE2–Nb–H1T	102(2)	96(2)
CE2–Nb–H2T	102(2)	102(2)
H1T–Nb–H2T	107(3)	120(3)
E–Nb–CE1	113.1(2)	112.0(3)
E–Nb–CE2	108.7(2)	108.5(3)
E–Nb–H1T	56(2)	65(2)
E–Nb–H2T	51(2)	55(2)
Nb–E–C17	118.9(2)	119.3(3)
Nb–E–C23	113.5(2)	115.1(2)
Nb–E–C29	115.4(2)	115.6(3)
C17–E–C23	99.7(3)	98.7(4)
C17–E–C29	102.8(3)	102.2(4)
C23–E–C29	104.3(3)	103.3(4)

^a E = Ge (**2**), Sn (**11**), and CE1 and CE2 are the centroids of the C1···C5 and C9···C13 cyclopentadienyl rings, respectively.

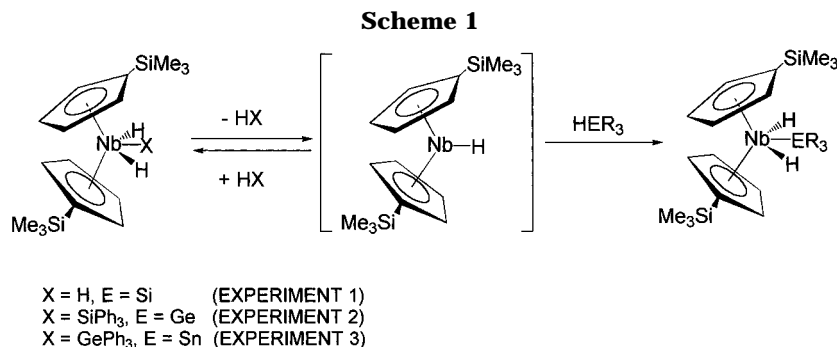
range for the values retrieved from the Cambridge Structural Database System (CSDS) files,⁸ are not considered to be significantly different. To our knowledge, the germyl complex is the first structurally characterized complex with a Nb–Ge bond. The Nb–Sn bond length agrees very well with the mean value retrieved from CSDS (2.833(9) Å). On the basis of the Nb, Si, Ge, and Sn covalent radii (1.34, 1.11, 1.22, and 1.41 Å, respectively), we can hypothesize that the Nb–E bond strengths are in following order Nb–Sn > Nb–Ge > Nb–Si ($d_{\text{obs}} = 2.830(1)$ (**11**), 2.710(1) (**2**), 2.616(3) Å; $d_{\text{calc}} = 2.75$, 2.56, and 2.45 Å; $\Delta(d_{\text{obs}} - d_{\text{calc}}) = 0.08$, 0.15, and 0.17 Å in **11**, **2**, and Nb(η^5 -C₅H₄SiMe₃)₂-(H)₂(SiPh₂H),⁴ respectively). The coordination around the E atoms shows a distorted tetrahedral geometry due to the steric hindrance between the Ph···Ph and the Ph···Cp' rings.

Reactivity of Niobocene Complexes with –SiPh₃, –GePh₃, and –SnPh₃ Moieties. A toluene solution of **12** reacts at room temperature with CO (1 atm) over 48 h to give the hydride–carbonyl complex Nb(η^5 -C₅H₄-SiMe₃)₂(H)(CO)⁹ and HSiPh₃ in 100% yield. No reaction of **2** and **11** with CO, under similar experimental

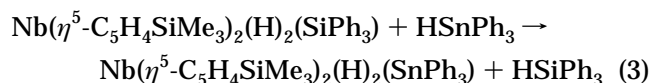
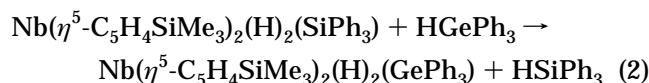
(7) Wilson, R. D.; Koetzle, T. F.; Hart, D. W.; Kwick, A.; Tipton, D. L.; Bau, R. *J. Am. Chem. Soc.* **1977**, *99*, 1775.

(8) Allen, F. H.; Bellard, S.; Brice, M. D.; Cartwright, B. A.; Doubleday, A.; Higgs, H.; Hummelink, T.; Hummelink-Peters, B. G.; Kennard, O.; Motherwell, W. *Acta Crystallogr., Sect. B* **1979**, *35*, 2331.

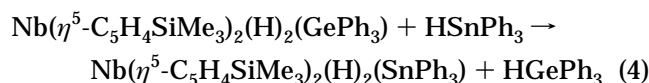
(9) Antiñolo, A.; Fajardo, M.; Jalón, F.; López-Mardomingo, C.; Otero, A.; Sanz-Bernabé, C. *J. Organomet. Chem.* **1989**, *369*, 187.



conditions, was observed after 48 h. A similar behavior was found in the reactions with CN(2,6-Me₂C₆H₃). Thus, **12** reacts with this isonitrile in toluene to give, over 48 h at room temperature, the hydride–isonitrile derivative Nb(η^5 -C₅H₄SiMe₃)₂(H)(CN(2,6-Me₂C₆H₃))¹⁰ and HSiPh₃ in 100% yield, while no reaction was observed with **2** and **11**. These results indicate that complex **12** is more reactive toward CO and CN(2,6-Me₂C₆H₃) than complexes **2** and **11**. Furthermore, it is noteworthy that the reaction of **12** with these π -acid ligands proceeds with elimination of HSiPh₃, without insertion, to give a silaacyl derivative, as found previously for other d⁰ M–Si bonds.^{1c–g,i,6c} Hydrogenolysis reactions were also studied. These reactions provide convenient routes to the corresponding hydrides from the appropriate d⁰ transition metal alkyl and silyl derivatives.^{1a,e,11} Thus, the silyl complex **12** reacts at room temperature with hydrogen (3 atm) in toluene over 48 h to afford the trihydride derivative **1** in 30% yield along with HSiPh₃. In contrast, no reaction was observed for **2** and **11** under similar experimental conditions. These results indicate that the Nb–Si bond is more reactive toward hydrogenolysis than the Nb–Ge and Nb–Sn bonds in these complexes. Finally, the reactivity of silyl-, germyl-, or stannyl-containing niobocene complexes toward the HEPH₃, E = Si, Ge, Sn, reagents in σ -bond metathesis reactions of d⁰ Nb–E bonds with E–H σ bonds have been studied. The reactions were monitored by ¹H NMR spectroscopy. Complex **12** reacts at 40 °C with HGePh₃ or HSnPh₃ over 1.5 h in toluene-*d*₈ solution to afford the σ -bond metathesis products **2** or **11** and HSiPh₃, respectively (eq 2 and 3; 100% conversion in both processes). In addition, a similar σ -bond metathesis



reaction was observed when **2** was heated at 75 °C with HSnPh₃ over 1.5 h in toluene-*d*₈ solution (eq 4; 100% conversion). However, no reaction was found, under



(10) Antiñolo, A.; Carrillo-Hermosilla, F.; Fajardo, M.; García-Yuste, S.; Otero, A.; Camanyes, S.; Maseras, F.; Moreno, M.; Lledós, A.; Lluch, J. M. *J. Am. Chem. Soc.* **1997**, *119*, 6107.

Table 2

experiment	10 ⁴ k _{app} (s ⁻¹)	T (K)	E _a (kcal mol ⁻¹)	ΔH [‡] (kcal mol ⁻¹)	ΔS [‡] (kcal mol ⁻¹ K ⁻¹)
1	5	333	23.9	23.3	3.10 ⁻³
	3	328			
	2	323			
	0.1	318			
	0.5	313			
2	16	333	27.6	26.9	9.10 ⁻³
	9	328			
	5	323			
	2	318			
	1	313			
3	4	363	36.1	35.3	23.10 ⁻³
	2	358			
	0.7	353			
	0.6	351			
	0.5	348			

analogous experimental conditions, between **2** and HSiPh₃ or between **11** and HSiPh₃ or HGePh₃.

Kinetic studies on these σ -bond metathesis processes have been carried out by following the reactions as a function of time and temperature by ¹H NMR spectroscopy. The experiments using **1**, **2**, and **12** with HEPH₃ were carried out under pseudo-first-order conditions, with respect to the niobocene species, by using a high initial concentration of HEPH₃.¹² Values of the apparent pseudo-first-order rate constants, k_{app}, at five temperature values were obtained for the different processes. The k_{app} values satisfactorily fit the Arrhenius plot, k_{app} = A exp(-E_a/RT), and the E_a values for the different reactions were calculated (Table 2). The Eyring plot, ln(k_{app}/T) against 1/T (k_{app} = (kT/h)exp(-ΔH[‡]/RT)exp(ΔS[‡]/R)), gives the activation parameters ΔH[‡] and ΔS[‡] for the different reactions (Table 2). A possible mechanism for these processes is shown in Scheme 1, which corresponds to a consecutive reaction with a reversible step.⁴ This mechanism was previously proposed for the reactions of **1** with several π -acid ligands and olefins, i.e., reaction of **1** with styrene to give the corresponding hydride–styrene species.¹⁴ A similar mechanism was also proposed¹⁵ for a ligand-displacement process in

(11) (a) Jordan, R. F.; Bajgur, C. S.; Dasher, W. E.; Rheingold, A. L. *Organometallics* **1987**, *6*, 1042. (b) Wochner, F.; Brintzinger, H. H. *J. Organomet. Chem.* **1986**, *309*, 65. (c) Gell, K. I.; Posin, B.; Schwartz, J.; Williams, G. M. *J. Am. Chem. Soc.* **1982**, *104*, 1846. (d) Lin, Z.; Marks, T. J. *J. Am. Chem. Soc.* **1987**, *109*, 7979.

(12) See, for example: (a) Espenson, J. H. *Chemical Kinetics and Reaction Mechanisms*, 1st ed.; McGraw-Hill: New York, 1981; p 76. (b) Wilkins, R. G. *Kinetics and Mechanism of Reactions of Transition Metal Complexes*, 2nd ed.; VCH: Weinheim, 1991; p 11.

(13) See, for example: (a) Kemp, W. *NMR in Chemistry. A Multi-nuclear Introduction*; McMillan: London, 1986. (b) Sandström, J. *Dynamic NMR Spectroscopy*; Academic Press: London, 1982.

(14) Antiñolo, A.; Carrillo, F.; García-Yuste, S.; Otero, A. *Organometallics* **1994**, *13*, 2761.

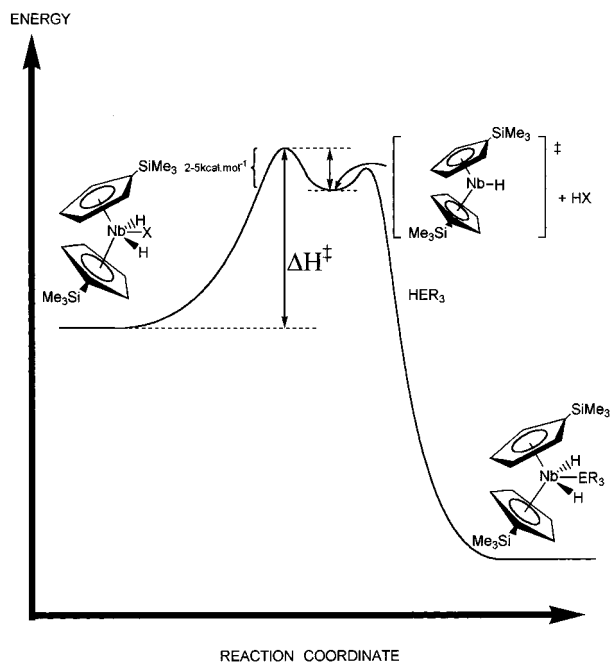


Figure 2. Energy diagram for the σ -bond metathesis processes.

cobalt complexes. It is noteworthy that for analogous metathesis processes of group 4 d^0 M–E σ -bonds,^{6c} concerted four-center transition states have been proposed. However, in the group 5 d^0 niobocenes, this is not possible since an empty orbital is not available on the niobium center to form the σ -bond metathesis transition state.

Absolute bond dissociation enthalpies are typically difficult to determine. One technique for determining a limit for absolute bond dissociation enthalpies by kinetic methods involves measuring ΔH^\ddagger for a reaction, such as that proposed in Scheme 1. If the barrier for the reverse reaction is sufficiently low, perhaps between 2 and 5 kcal mol⁻¹, ΔH^\ddagger provides a reasonable estimate for the bond-dissociation energies.¹⁶ This is shown schematically in the energy diagram of Figure 2.

Since the appropriate X–H bond strengths are known, we can use ΔH^\ddagger to estimate the Nb–X bond dissociation enthalpies. Thus, from experiment 1 (see Scheme 1), assuming that ΔH^\ddagger corresponds (in accordance with the proposed mechanism) to the dissociation of two Nb–H bonds and the consequent formation of an H₂ molecule, eq 5 allows us to estimate the value of mean bond-dissociation enthalpy of the Nb–H bond, $D(\text{Nb–H})$, as 63.8 kcal mol⁻¹, using a value of 104 kcal mol⁻¹ for the bond dissociation enthalpy of H₂, $D(\text{H}_2)$.¹⁷

$$\Delta H_1^\ddagger \approx 2D(\text{Nb–H}) - D(\text{H}_2) \quad (5)$$

Likewise, the bond dissociation enthalpies for the Nb–Si, $D(\text{Nb–Si})$, and Nb–Ge bonds, $D(\text{Nb–Ge})$, can be estimated from eqs 6 and 7, which correspond to experiments 2 and 3, respectively (see Scheme 1), using

the following values:¹⁸ $D(\text{Nb–H}) = 63.8$ kcal mol⁻¹, $D(\text{Si–H}) = 90$ kcal mol⁻¹, and $D(\text{Ge–H}) = 82$ kcal mol⁻¹.

$$\Delta H_2^\ddagger \approx D(\text{Nb–H}) + D(\text{Nb–Si}) - D(\text{Si–H}) \quad (6)$$

$$\Delta H_3^\ddagger \approx D(\text{Nb–H}) + D(\text{Nb–Ge}) - D(\text{Ge–H}) \quad (7)$$

Bond dissociation enthalpies of 53.3 and 53.6 kcal mol⁻¹ are found for Nb–Si and Nb–Ge, respectively, indicating that a similar bond strength for both Nb–E bonds in complexes **12** and **2** must be considered.

Because complex **11** (see experiment 3, Scheme 1) results from an irreversible reaction of **1**, **2**, or **12** with HSnPh₃, it was not possible to evaluate the value of $D(\text{Nb–Sn})$ by using the equilibrium method. However, if we consider the term ΔH as the major contribution in the equation $\Delta G = \Delta H - T\Delta S$, because ΔS is lower, we can evaluate $D(\text{Nb–Sn})$ from eq 8. Thus, ΔH_3 , the

$$\Delta H_3 \approx D(\text{Nb–Ge}) + D(\text{Nb–H}) + D(\text{Sn–H}) - D(\text{Nb–Sn}) - D(\text{Nb–H}) - D(\text{Ge–H}) \quad (8)$$

enthalpy for the reaction in eq 4, must be <0 in a irreversible process. With these considerations, a value of $D(\text{Nb–Sn}) > 45$ kcal mol⁻¹ was obtained.

Thus, our analysis was focused on bond-dissociation enthalpies, considering the same $D(\text{Nb–H})$ value for the different niobocene complexes. Factors such as solvation energies essentially canceled, and a comparison of solution-phase Nb–E bond strengths with those of gas-phase E–H bonds have been made.¹⁹ Despite these disadvantages, the qualitative trends are clear. In conclusion, we have shown that the silyl-, germyl-, and stannyl-containing niobocene complexes have comparable $D(\text{Nb–E})$ values. However, the experimental results indicate the reactivity trend Nb–SiPh₃ > Nb–GePh₃ > Nb–SnPh₃ for the σ -bond metathesis processes. This behavior can be rationalized in terms of differences in reactant and product bond strengths (see Scheme 1). Thus, in experiment 1, the energy required to break two Nb–H bonds is supplied by formation of a strong H–H bond and a similar driving force is likely to account for the results of experiments 2 and 3, where the energy required to break the Nb–H and Nb–Si or Nb–Ge bonds is compensated by formation of relatively strong H–Si and H–Ge bonds. This explanation has been postulated by Tilley et al.^{6c} to rationalize the reactivity trends of silyl, germyl, and stannyl d^0 zirconocene complexes in σ -bonds metathesis reactions which parallel those found in the niobium system. In an analogous way, the reactivity trend observed for the complexes in the hydrogenolysis processes can be rationalized.

Concluding Remarks

This study has revealed that niobocene germyl and stannyl hydrides Nb(η^5 -C₅H₄SiMe₃)₂(H)₂(ER₃), E = Ge, Sn, can be easily prepared from reaction of the trihy-

(15) Janowicz, A. H.; Bryndza, H. E.; Bergman, R. G. *J. Am. Chem. Soc.* **1981**, *103*, 1516.

(16) Stoutland, P. O.; Bergman, R. G.; Nolan, S. P.; Hoff, C. D. *Polyhedron* **1988**, *7*, 1429.

(17) Berkowitz, J.; Ellison, G. B.; Gutman, D. *J. Phys. Chem.* **1994**, *98*, 2744.

(18) Bond dissociation enthalpies $D(\text{Si–H})$ and $D(\text{Ge–H})$ were estimated in the compounds Me₃E–H: Jackson, R. A. *J. Organomet. Chem.* **1979**, *166*, 17.

(19) (a) Martinho Simoes, J. A.; Beauchamp, J. L. *Chem. Rev.* **1990**, *90*, 629. (b) Schaller, C. P.; Cummins, C. C.; Wolczanski, P. T. *J. Am. Chem. Soc.* **1996**, *118*, 591. (c) Jones, W. D.; Feher, F. J. *J. Am. Chem. Soc.* **1984**, *106*, 1650.

drude $\text{Nb}(\eta^5\text{-C}_5\text{H}_4\text{SiMe}_3)_2(\text{H})_3$ with the appropriate HER_3 reagents. Reactivity studies on the $\text{Nb}(\eta^5\text{-C}_5\text{H}_4\text{SiMe}_3)_2\text{-}(\text{H})_2(\text{EPh}_3)$ species in hydrogenolysis and σ -bond metathesis processes indicate a reactivity trend $\text{Nb-SiPh}_3 > \text{Nb-GePh}_3 > \text{Nb-SnPh}_3$. On the basis of data obtained from a ^1H NMR study at different temperatures, bond-dissociation enthalpies, $D(\text{Nb-E})$, have been estimated for these species, and similar values were found for all complexes. The results indicate that the differences in product stabilities in the processes are probably responsible for the reactivity trend found.

Experimental Section

General Procedures. All operations were performed under an inert atmosphere using standard vacuum-line (Schlenk) techniques. Solvents were purified by distillation from the appropriate drying agents before use. NMR spectra were obtained on a Varian Unity FT-300 and Varian Gemini FT-200 instruments. IR spectra were recorded as Nujol mulls between CsI plates (in the region between 4000 and 200 cm^{-1}) on a Perkin-Elmer PE 883 IR spectrophotometer. Elemental analyses were performed on a Perkin-Elmer 2400 microanalyzer. $\text{Nb}(\eta^5\text{-C}_5\text{H}_4\text{SiMe}_3)_2(\text{H})_3$ was prepared as described earlier.²⁰

Preparation of $\text{Nb}(\eta^5\text{-C}_5\text{H}_4\text{SiMe}_3)_2(\text{H})_2(\text{GeR}_3)$ ($\text{GeR}_3 = \text{GePh}_3$ (2), GePh_2H (3), GeEt_3 (4), GeHexyl_3 (5), Ge^iAm_3 (6), $\text{GeHexyl}_2\text{Cl}$ (7), $\text{Ge}^i\text{Am}_2\text{Cl}$ (8), $\text{GeHexyl}_2\text{H}$ (9), $\text{Ge}^i\text{Am}_2\text{H}$ (10)). To a solution of $\text{Nb}(\eta^5\text{-C}_5\text{H}_4\text{SiMe}_3)_2(\text{H})_3$ (1; 300 mg, 0.81 mmol) in 25 mL of toluene was added R_3GeH (0.81 mmol) by syringe. The solution was warmed to $65\text{ }^\circ\text{C}$ and stirred for 3 h. The resulting solution was filtered and evaporated to dryness. The brown oily residue was extracted with 20 mL of ethanol. After concentration and cooling, white or pale crystals were obtained for compounds 2, 3, 7, and 8.

2: white crystals, 90% yield. IR (Nujol) $\nu(\text{Nb-H})$: 1760 cm^{-1} . ^1H NMR (200 MHz, C_6D_6): δ 0.04 (s, 18H, SiMe_3), 4.28 (m, 4H, C_5H_4), 5.00 (m, 4H, C_5H_4), 7.50 (m, 15H, GePh_3), -3.48 (s, 2H, Nb-H). ^{13}C NMR (300 MHz, C_6D_6): δ 0.14 (SiMe_3), 97.81 (C_1), 92.30, 95.51 (C_5H_4), 126.50, 129.41, 135.98, 150.63 (GePh_3). Anal. Calcd for $\text{C}_{34}\text{H}_{43}\text{NbSi}_2\text{Ge}$: C, 60.66; H, 6.39. Found: C, 60.34; H, 6.07.

3: white crystals, 81% yield. IR (Nujol) $\nu(\text{Nb-H})$: 1759 cm^{-1} . ^1H NMR (200 MHz, C_6D_6): δ 0.13 (s, 18H, SiMe_3), 4.14 (m, 4H, C_5H_4), 4.94 (m, 4H, C_5H_4), 7.30 (m, 15H, GePh_2H), 5.81 (s, 1H, GePh_2H), -3.69 (s, 2H, Nb-H). ^{13}C NMR (300 MHz, C_6D_6): δ 0.21 (SiMe_3), 98.60 (C_1), 91.10, 94.47 (C_5H_4), 127.32, 131.18, 134.6, 148.3 (GePh_2H). Anal. Calcd for $\text{C}_{28}\text{H}_{39}\text{NbSi}_2\text{Ge}$: C, 56.32; H, 6.54. Found: C, 56.22; H, 6.32.

4: brown oil, 85% yield. IR (Nujol) $\nu(\text{Nb-H})$: 1740 cm^{-1} . ^1H NMR (200 MHz, C_6D_6): δ 0.12 (s, 18H, SiMe_3), 4.35 (m, 4H, C_5H_4), 4.95 (m, 4H, C_5H_4), 0.90 (q, 6H, $\text{Ge}(\text{CH}_2\text{CH}_3)_3$), 1.30 (t, 9H, $\text{Ge}(\text{CH}_2\text{CH}_3)_3$), -4.46 (s, 2H, Nb-H). ^{13}C NMR (300 MHz, C_6D_6): δ 0.43 (SiMe_3), 94.82 (C_1), 90.69, 93.11 (C_5H_4), 13.99 ($\text{Ge}(\text{CH}_2\text{CH}_3)_3$), 10.73 ($\text{Ge}(\text{CH}_2\text{CH}_3)_3$).

5: brown oil, 81% yield. IR (Nujol) $\nu(\text{Nb-H})$: 1731 cm^{-1} . ^1H NMR (200 MHz, C_6D_6): δ 0.16 (s, 18H, SiMe_3), 4.43 (m, 4H, C_5H_4), 5.02 (m, 4H, C_5H_4), 1.40 (m, 30H, $\text{Ge}((\text{CH}_2)_5\text{CH}_3)_3$), 0.92 (t, 9H, $\text{Ge}((\text{CH}_2)_5\text{CH}_3)_3$), -4.33 (s, 2H, Nb-H). ^{13}C NMR (300 MHz, C_6D_6): δ 0.90 (SiMe_3), 95.13 (C_1), 91.27, 93.73 (C_5H_4), 14.90, 23.7, 27.5, 32.81, 34.95 ($\text{Ge}((\text{CH}_2)_5\text{CH}_3)_3$), 13.10 ($\text{Ge}((\text{CH}_2)_5\text{CH}_3)_3$).

6: brown oil, 81% yield. IR (Nujol) $\nu(\text{Nb-H})$: 1724 cm^{-1} . ^1H NMR (200 MHz, C_6D_6): δ 0.15 (s, 18H, SiMe_3), 4.41 (m, 4H, C_5H_4), 5.00 (m, 4H, C_5H_4), 1.08-1.60 (m, 33H, Ge^iAm_3), -4.34

(s, 2H, Nb-H). ^{13}C NMR (300 MHz, C_6D_6): δ 0.52 (SiMe_3), 94.61 (C_1), 90.84, 93.27 (C_5H_4), 22.35, 22.94, 31.14, 32.08, 41.01 (Ge^iAm_3).

7: pale pink crystals, 70% yield. IR (Nujol) $\nu(\text{Nb-H})$: 1736 cm^{-1} . ^1H NMR (200 MHz, C_6D_6): δ 0.14 (s, 18H, SiMe_3), 4.80 (m, 4H, C_5H_4), 5.11 (m, 4H, C_5H_4), 1.35 (m, 20H, $\text{Ge}((\text{CH}_2)_5\text{CH}_3)_2\text{Cl}$), 0.38 (t, 6H, $\text{Ge}((\text{CH}_2)_5\text{CH}_3)_2\text{Cl}$), -3.89 (s, 2H, Nb-H). ^{13}C NMR (300 MHz, C_6D_6): δ 0.95 (SiMe_3), 98.64 (C_1), 92.9, 95.06 (C_5H_4), 23.48, 26.71, 32.46, 32.63, 34.07 ($\text{Ge}((\text{CH}_2)_5\text{CH}_3)_2\text{Cl}$), 14.89 ($\text{Ge}((\text{CH}_2)_5\text{CH}_3)_2\text{Cl}$). Anal. Calcd for $\text{C}_{28}\text{H}_{54}\text{NbSi}_2\text{-GeCl}$: C, 54.85; H, 8.98. Found: C, 54.68; H, 8.77.

8: pale pink crystals, 73% yield. IR (Nujol) $\nu(\text{Nb-H})$: 1757 cm^{-1} . ^1H NMR (200 MHz, C_6D_6): δ 0.14 (s, 18H, SiMe_3), 4.49 (m, 4H, C_5H_4), 5.11 (m, 4H, C_5H_4), 0.60-1.60 (m, 22H, $\text{Ge}^i\text{Am}_2\text{Cl}$), -3.89 (s, 2H, Nb-H). ^{13}C NMR (300 MHz, C_6D_6): δ 0.90 (SiMe_3), 98.63 (C_1), 92.88, 95.06 (C_5H_4), 23.09, 31.74, 29.61, 35.62 ($\text{Ge}^i\text{Am}_2\text{Cl}$). Anal. Calcd for $\text{C}_{26}\text{H}_{50}\text{NbSi}_2\text{-GeCl}$: C, 53.37; H, 8.72. Found: C, 53.61; H, 8.63.

9: brown oil, 78% yield. IR (Nujol): $\nu(\text{Nb-H})$ 1717 cm^{-1} , $\nu(\text{Ge-H})$ 1913 . ^1H NMR (200 MHz, C_6D_6): δ 0.17 (s, 18H, SiMe_3), 4.26 (m, 4H, C_5H_4), 4.49 (m, 4H, C_5H_4), 1.38 (m, 20H, $\text{Ge}((\text{CH}_2)_5\text{CH}_3)_2\text{H}$), 0.82 (t, 6H, $\text{Ge}((\text{CH}_2)_5\text{CH}_3)_2\text{H}$), -4.32 (s, 2H, Nb-H). ^{13}C NMR (300 MHz, C_6D_6): δ 0.89 (SiMe_3), 96.21 (C_1), 91.25, 93.72 (C_5H_4), 23.40, 27.91, 32.29, 33.19, 34.07 ($\text{Ge}((\text{CH}_2)_5\text{CH}_3)_2\text{H}$), 14.82 ($\text{Ge}((\text{CH}_2)_5\text{CH}_3)_2\text{H}$).

10: brown oil, 82% yield. IR (Nujol): $\nu(\text{Nb-H})$ 1749 cm^{-1} , $\nu(\text{Ge-H})$ 1907 . ^1H NMR (200 MHz, C_6D_6): δ 0.16 (s, 18H, SiMe_3), 4.26 (m, 4H, C_5H_4), 4.98 (m, 4H, C_5H_4), 0.80-1.65 (m, 22H, $\text{Ge}^i\text{Am}_2\text{H}$), -4.37 (s, 2H, Nb-H). ^{13}C NMR (300 MHz, C_6D_6): δ 0.96 (SiMe_3), 96.35 (C_1), 91.17, 93.25 (C_5H_4), 23.35, 32.00, 20.79, 36.94 ($\text{Ge}^i\text{Am}_2\text{H}$).

$\text{Nb}(\eta^5\text{-C}_5\text{H}_4\text{SiMe}_3)_2(\text{H})_2(\text{SnPh}_3)$ (11). To a solution of $\text{Nb}(\eta^5\text{-C}_5\text{H}_4\text{SiMe}_3)_2(\text{H})_3$ (1; 300 mg, 0.81 mmol) in 25 mL of toluene was added Ph_3SnH (0.81 mmol) by syringe. The solution was warmed to $65\text{ }^\circ\text{C}$ and stirred for 3 h. The resulting solution was filtered and evaporated to dryness. The oily residue was extracted with 20 mL of ethanol. After concentration and cooling, white crystals were obtained.

11: white crystals, 88% yield. IR (Nujol) $\nu(\text{Nb-H})$: 1756 cm^{-1} . ^1H NMR (200 MHz, C_6D_6): δ 0.01 (s, 18H, SiMe_3), 4.34 (m, 4H, C_5H_4), 4.96 (m, 4H, C_5H_4), 7.50 (m, 15H, SnPh_3), -4.44 (s, 2H, Nb-H). ^{13}C NMR (300 MHz, C_6D_6): δ 0.193 (SiMe_3), 95.92 (C_1), 90.34, 92.75 (C_5H_4), 127.84, 128.00, 137.46, 149.62 (SnPh_3). Anal. Calcd for $\text{C}_{34}\text{H}_{43}\text{NbSi}_2\text{Sn}$: C, 56.76; H, 5.98. Found: C, 56.26; H, 5.90.

Kinetics of the Reaction of 1 with HSiPh_3 (Experiment 1). Determination of First-Order Rate Constants. A measured amount of 1 (24 mg) was dissolved in toluene- d_8 in a 5-mm-NMR tube, and HSiPh_3 (166 mg) was added. The final volume was 0.8 mL. The concentration of 1 was 0.08 M, and the molar ratio of 1: HSiPh_3 was 1:10. The tube was vigorously shaken for about 5 s and then placed into the spectrometer. Each spectrum recorded at 313 K was the result of coadding 16 transients which required nearly 1 min to acquire. Spectra were automatically recorded every 10 min using the kinetic analysis software from Varian. Variations of the intensity of the more intense peak from the pseudodoublet for the hydride ligands in 1 were measured for three $t_{1/2}$. A computer analysis method for intensities gives a straight-line segment in a plot of $\ln(\text{intensity})$ against time. The error is given by the standard deviation in the regression analysis. Similar experiments were carried out at 318, 323, 328, and 333 K.

Kinetics of the Reaction of 12 with HGePh_3 (Experiment 2). Determination of First-Order Rate Constants. A measured amount of 12 (40 mg) was dissolved in toluene- d_8 in a 5-mm-NMR tube, and HGePh_3 (190 mg) was added. The final volume was 0.8 mL. The concentration of 12 was 0.08 M, and the molar ratio of 12: HGePh_3 was 1:10. The tube was vigorously shaken for about 5 s and then placed into the spectrometer. Each spectrum recorded at 313 K was the result of coadding 16 transients which required nearly 1 min to

(20) Antiñolo, A.; Chaudret, B.; Commenges, G.; Fajardo, M.; Jalon, F.; Morris, R. H.; Otero, A.; Schweitzer, C. T. *J. Chem. Soc., Chem. Commun.* **1988**, 1210.

Table 3. Summary of Crystal Data for Compounds 2 and 11

	2	11
formula	C ₃₄ H ₄₃ GeNbSi ₂	C ₃₄ H ₄₃ NbSi ₂ Sn
fw	673.38	
cryst syst		monoclinic
space group		<i>P</i> 2 ₁ / <i>n</i>
diffractometer		Philips PW 1100
radiation		(Mo K α), $\lambda = 0.710\ 73\ \text{\AA}$
monochromator		graphite
temp, K		293
<i>a</i> , \AA	13.336(3)	13.547(4)
<i>b</i> , \AA	22.403(5)	22.459(8)
<i>c</i> , \AA	11.344(3)	11.448(4)
β , deg	98.47(2)	99.00(2)
<i>V</i> , \AA^3	3352(1)	3440(2)
<i>Z</i>		4
<i>D</i> _{calcd} , g cm ⁻³	1.334	1.389
<i>F</i> (000)	1392	1464
cryst dimens, mm	0.25 × 0.30 × 0.35	0.20 × 0.25 × 0.30
μ (Mo K α), cm ⁻¹	13.30	11.49
2 θ range, deg	6–48	6–44
reflns measd, range <i>h, k, l</i>	0/15,0/25,-12/12	-16/15,0/26,0/13
total no. of unique data	4042 ($F_o \geq -\sigma(F_o^2)$)	4206 ($F_o^2 \geq -3\sigma(F_o^2)$)
no. of unique obsd data ($F_o \geq 4\sigma(F_o)$)	2264	1964
data/restraints/params	4042/0/354	4206/0/354
goodness of fit ^a	1.089	0.785
R1 ^b	0.0352	0.0403
wR2 ^c	0.0894	0.0755
weighting scheme, <i>a, b</i> ^d	0.0176, 0.0000	0.0131, 0.0000

^a GOOF = $[\sum[w(F_o^2 - F_c^2)^2]/(n - p)]^{1/2}$. ^b R1 = $\sum||F_o| - |F_c||/\sum|F_o|$. ^c wR2 = $[\sum[w(F_o^2 - F_c^2)^2]/\sum[w(F_o^2)^2]]^{1/2}$. ^d $w = 1/[\sigma^2(F_o^2) + (aP)^2 + bP]$, where $P = [\max(F_o^2, 0) + 2F_c^2]/3$.

acquire. Spectra were automatically recorded every 10 min using the kinetic analysis software from Varian. Variations of the intensity of the singlet peak for the hydride ligands in **12** were measured for three $t_{1/2}$. A computer analysis method for intensities gives a straight-line segment in a plot of ln-(intensity) against time. The error is given by the standard deviation in the regression analysis. Similar experiments were carried out at 318, 323, 328, and 333K.

Kinetics of the Reaction of 2 with HSnPh₃ (Experiment 3). Determination of First-Order Rate Constants. A measured amount of **2** (43 mg) was dissolved in toluene-*d*₈ in a 5-mm-NMR tube, and HSnPh₃ (224 mg) was added. The final volume was 0.8 mL. The concentration of **2** was 0.08 M, and the molar ratio of **2**:HSnPh₃ was 1:10. The tube was vigorously shaken for about 5 s and then placed into the spectrometer. Each spectrum recorded at 348 K was the result of coadding 16 transients which required nearly 1 min to acquire. Spectra were automatically recorded every 10 min using the kinetic analysis software from Varian. Variations of the intensity of the singlet peak for the hydride ligands in **2** were measured for three $t_{1/2}$. A computer analysis method for intensities gives a straight-line segment in a plot of ln-(intensity) against time. The error is given by the standard deviation in the regression analysis. Similar experiments were carried out at 351, 353, 358, and 363K.

X-ray Data Collection, Structure Determination, and Refinement of Complexes 2 and 11. Suitable crystals were sealed in Lindemann capillaries under dry nitrogen and used for data collection. The crystallographic data are summarized in Table 3. Accurate unit-cell parameters were determined

by least-squares refinement of the setting angles of 24 randomly distributed and carefully centered reflections with θ in the range 8–15° (**2**) and 10–17° (**11**). The data collections were performed by the $\theta/2\theta$ scan mode, at 293 K, with a variable scan speed of 3–9.6 and 1.2–4.8 deg min⁻¹ for **2** and **11**, respectively, and a scan width of 1.20 + 0.34 tan θ for both. One standard reflection was monitored every 100 measurements; no significant decay was noticed over the course of data collection. The individual profiles were analyzed following the method of Lehmann and Larsen.²¹ Intensities were corrected for Lorentz and polarization effects and reduced to F_o^2 . The structures were solved by direct methods (SIR92²²) and refined by full-matrix least-squares on F^2 using SHELXL-93,²³ first with isotropic thermal parameters and then with anisotropic thermal parameters for all the non-hydrogen atoms. The niobium hydrides were clearly located in the ΔF maps and refined isotropically. All of the other hydrogen atoms were placed at their geometrically default-distance calculated positions and refined riding on their parent carbon atoms with three common isotropic displacement parameters for the H_{Cp}, H_{Ph}, and H_{Me} atoms, respectively. After the final cycles of refinement, no parameters shifted by more than 0.009 Å (for H2T) in **2** and 0.011 Å for H1T in **11** and the max and mean shift/esd deviations were 0.105 for y (H2T) and 0.007 in **2** and -0.204 for z (H1T) and 0.013 in **11**, respectively. The final difference Fourier maps showed no residual density outside -0.79 and 1.12 and -0.56 and 0.68 e/Å³ in **2** and **11**, respectively. All calculations were carried out on the GOULD POWERNODE 6040 and ENCORE 91 of the Centro di Studio per la Strutturistica Diffrattometrica del CNR, Parma. The Parst²⁴ and ORTEP²⁵ programs were also used. The final atomic coordinates are provided in the Supporting Information.

Acknowledgment. A.A., F.C.-H., M.F., J.F.-B., A.O., and E.V. gratefully acknowledge financial support from the Dirección General de Enseñanza Superior (DGES) (Grant No. PB 95-0023-CO1) of Spain, and M.L. and M.A.P. gratefully acknowledge financial support from the Ministero dell'Università e della Ricerca Scientifica e Tecnologica (MURST) and Consiglio Nazionale delle Ricerche (CNR) (Rome, Italy). We thank also several commentaries from Prof. R. Andersen, Berkeley University.

Supporting Information Available: Tables of final atomic coordinates for the non-hydrogen atoms (Tables SI, SII) and hydrogen atoms (Tables SIII, SIV), anisotropic thermal parameters (Tables SV, SVI), complete bond distances and angles (Tables SVII, SVIII), and complete crystallographic data (Tables SIX, SX) (14 pages). Ordering information is given on any current masthead page.

OM971001B

(21) Lehman, M. S.; Larsen, F. K. *Acta Crystallogr., Sect. A* **1974**, *30*, 580.

(22) Altomare, A.; Cascarano, G.; Giacovazzo, C.; Guagliardi, A.; Burla, M. C.; Polidori, G.; Camalli, M. *J. Appl. Crystallogr.* **1994**, *27*, 580.

(23) Sheldrick, G.M. *SHELXL-93. Program for the refinement of crystal structures*; University of Göttingen: Göttingen, Germany, 1993.

(24) Nardelli, M. *Comput. Chem.* **1983**, *7*, 95.

(25) Johnson, C. K. *ORTEP*. Report ORNL-3794; Oak Ridge National Laboratory: Oak Ridge, TN, 1965.